Bull. Chem. Soc. Ethiop. **2025**, 39(7), 1317-1334.
DOI: https://dx.doi.org/10.4314/bcse.v39i7.7

ISSN 1011-3924
Printed in Ethiopia
Online ISSN 1726-801X

SYNTHESIS, CHARACTERIZATION AND EVALUATION OF ANTICANCER AND ANTIOXIDANT ACTIVITY OF NEW AZO DYE DERIVATIVES FROM TRYPTAMINE AND COMPLEXES

Vian Yamin Jirjees[1*] and Abbas Ali Salih Al –Hamdani[2*]

[1]Department of Chemistry, College of Science, University of Dohuk, Kurdistan Region, Iraq
[2]Department of Chemistry, College of Science for Women, University of Baghdad, Iraq

(Received February 10, 2025; Revised March 13, 2025; Accepted March 17, 2025)

ABSTRACT. This new azo dye 3-((2-(1H-indol-3-yl) ethyl) diazenyl) quinoline-2-ol was subsequently used to prepare a series of complexes with the metal ions of Cr^{+3}, Cu^{+2}, VO^{+2}, $Mn^{+2}$and Mo^{+6}. The compounds identified by ^{1}H and ^{13}C-NMR, FT-IR, UV-Vis, mass spectroscopy, as well as TGA, DSC, and C.H.N., conductivity, magnetic susceptibility, metal and chlorine content. The results showed that the ligand behaves in a bidantate, and that the complexes gave octahedral, excepting for VO^{+2} square pyramid was given, that all complexes are non-electrolytes. The effectiveness of mention the compounds in inhibiting free radicals was evaluated by the ability to act as an antioxidant was measured using DPPH as a free radical and gallic acid as a standard substance, the IC_{50} value was determined, because the ligand was found to have a higher ability to inhibit free radicals, and the ability to inhibit the complexes varied according to the IC_{50} value. The anti-breast cancer efficacy of the compounds was evaluated at five concentrations each, the results showed that the IC_{50} value for ligand was 49.86 µg/mL, while the Mo complex gave 25.48 µg/mL, Cu complex gave 123.8 µg/mL, meaning that the Mo-complex gave a higher inhibition value than ligand and Cu.

KEY WORDS: Antioxidant (DPPH), Azo dye complexes, Tryptamine, Thermal analysis, Anticancer

INTRODUCTION

Breast cancer is the most common type of cancer among women, often associated with the over expression of the estrogen receptor alpha (ERα). As a result, ERα is a crucial target for strategies aimed at preventing breast cancer. Tamoxifen, a stilbene-based compound, binds to the estrogen receptor and helps prevent the development of breast cancer. However, there is a growing need for new compounds to replace anti-hormone drugs like tamoxifen, as tumors can develop resistance to these treatments [1]. The indole nucleus is a core structure found in many natural heterocyclic compounds and has garnered significant attention in various fields such as industrial, agricultural, and medicinal chemistry [2, 3]. Tryptamine is an indole ring structure, which consists of a fused bicyclic system made up of a pyrrole ring and a benzene ring, connected to an amino group via a two-carbon side chain [4]. Azo dyes are organic compounds [5], that have been widely used in various fields, including textiles and medicine. Azo compounds are very important and have entered many fields, including agriculture, industry, and medicine, as well as their high biological effectiveness against fungi and bacteria, due to their containing the azo group [6, 7]. Aromatic azo compounds are generally more stable than aliphatic ones. Aromatic azo compounds are widely used in the production of synthetic organic compounds because they are stable compounds and have a wide range of colors including yellow, orange, red, brown, and blue [8]. On the other hand, aliphatic azo compounds are mainly used as radical initiators in the polymerization of alkanes to produce plastics [9, 10]. Coordination compounds represent a significant and complex field in modern inorganic chemistry [11]. These compounds arise when a ligand coordinates with a metal through two or more binding sites, leading to the formation of

*Corresponding authors. E-mail: vian.jirhees@uod.ac, abbasas_chem@csw.uobaghdad.edu.iq

a heterocyclic ring structure [12]. Through research, we did not find a previous study similar to our compound, according to a search in Science Finder. In this paper study is to mold the azo ligand into novel complexes of the metal ions Cr^{+3}, Cu^{+2}, V^{+4}, Mn^{+2} and Mo^{+6}. Their stability and thermal breakdown were investigated using DSC and TGA curves in addition to spectroscopic studies for characterization. Using the reference Gallic acid, we also assessed the antioxidant properties of the all by using the DPPH radical. Five concentrations of ligand, Cu and Mo complexes were used in a study to assess their anticancer potential against MCF-7, and the IC_{50} was calculated.

EXPERIMENTAL

Material and methods

All of the materials tryptamine, 2-hydroxyquinoline, $NaNO_2$, NaOH, $VOSO_4.5H_2O$, $MnCl_2.4H_2O$, $CrCl_3.6H_2O$ $CuCl_2.2H_2O$, and $(NH_4)_2MoO_4$ were obtained from Sigma Aldrich and ethanol, HCl conc. and DMSO from Merck. The single-V.3.O-single Euro vector model EA/3000 has been utilized. To achieve (C.H.N.) analysis, metal ions were calculated as chloride using a gravimetric approach. Molar conductivity of the complexes were measured with a Conduct meter W.T.W. at room temperature in 1×10^{-3} M (DMSO). Mass spectra (MS) QP50A: DI Analysis ShimadzuQP-2010-Plus (E170Ev), electron impact (30 eV) spectrometer was logged for the complexes. The UV-Vis absorption spectra to the (200–1100 nm) range were obtained using the UV-1800 Shimadzu Spectrophotometer, 10^{-3} M solutions in DMSO at room temperature. For thermo gravimetric analysis, studies were carried out using the Perkin-Elmer Pyris Diamond TGA-DSC and Fourier transform was examined using the IR Prestige-21 to study FT-IR spectra. Metals were identified using a Shimadzu (F.A.A.) 680 G atomic clock. ^{1}H and ^{13}C nuclear magnetic resonance spectra were recorded utilizing the Bruker spectrometer operating at a frequency of 400 MHz. spectrometer.

Synthesis of {3-[2-(1H-indol-2-yl)ethyldiazenyl)quinolin-2-ol] (HL)

Tryptamine (1 g, 6.250 mmol) was dissolved in 15 mL of ethanol, and 3 mL of 37% HCl conc. was added at 0-5 °C while being refrigerated. Then, (0.43 g, 6.250 mmol) of $NaNO_2$ was gradually added, ensuring the temperature did not exceed 5 °C. The solution was stirred for approximately 60 min, leading to the formation of the diazonium salt. Separately, 2-hydroxyquinoline (1 g, 6.250 mmol) was dissolved in 15 mL of ethanol, and the diazonium salt solution was added. Following this, 3 mL of 1 M sodium hydroxide solution was introduced, resulting in the precipitation of a dark green azo compound. This was weighed after being filtered, collected, and given time to dry. Its melting point was 105-110 °C, and its yield was 84.5%. Figure 1 shows the ^{1}H-NMR and ^{13}C-NMR spectra of the free azo ligand was dissolved in (DMSO-d_6 ppm) solvent using tetramethylsilane as the internal standard. Shows multiple distinct signals at δ (1.90 ppm) is attributed to (4H) t, CH_2-CH_2, 2.69 ppm DMSO, 6.5-6.8 ppm (1H) s, CH-NH indole), 7.56-8.56 ppm (4H) m, CH arom. 8.58-8.93 ppm (1H) d, CH-N=N, 9.75-10.39 ppm (1H) s, OH arom respectively. In the ^{13}C-NMR, Figure 1 shows signals at (C1) 169.75, (C2) 118, (C3) 181.97, (C4) 165.30, (C5) 132.21, (C6) 137.27, (C7) 148.96, (C8) 145.00, (C9) 157.23, (C10) 33.6, (C11) 49.71, (C12) 127.48, (C13) 172.74, (C14) 106.9, (C15) 189.75, (C16) 196.20, (C17) 178.10, (C18) 172.74, (C19) 210 [13-16].

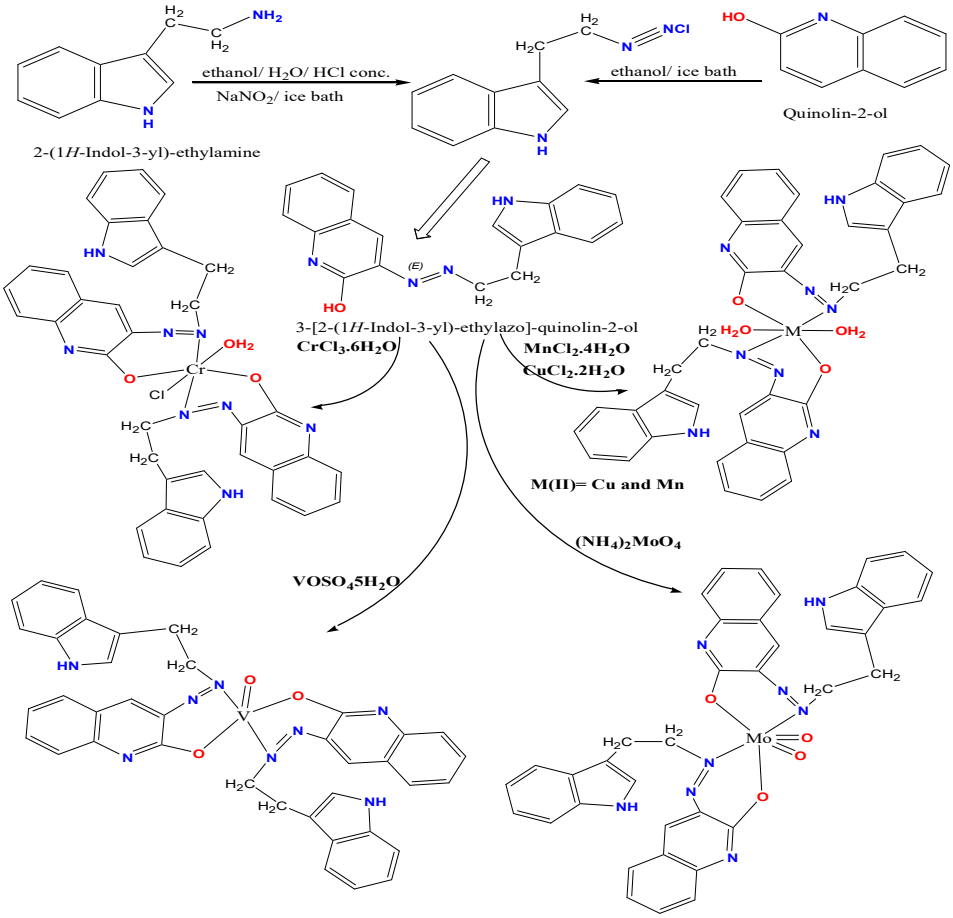

Scheme 1. Formation for the ligand (HL) and its metal complexes.

General approach for synthesis of metal complexes

The metal ions complexes for Cr^{+3}, Cu^{+2}, VO^{+2}, Mn^{+2} and Mo^{+6} were prepared using metal ions. As a stoichiometric amount of (1:2) M:L for $CrCl_3 \cdot 6H_2O$ (0.421 g, 1.581 mmol), $MnCl_2 \cdot 4H_2O$ (0.312 g, 1.581 mmol), $CuCl_2 \cdot 2H_2O$ (0.269 g, 1.581 mmol) chloride salts and $VOSO_4 \cdot 5H_2O$ (0.399 g, 1.581 mmol) and $(NH_4)_2$ MoO_4 (0.309 g, 1.581 mmol) dissolved in 20 mL distilled water was gradually added dropwise additions in round bottom flask, a stoichiometric amount of (1 g, 3.163 mmol) from azo day ligand, dissolved in 10 mL pure ethanol, was continually stirred. The combination was brought to between 40 and 50 °C for 2 hours reverse escalation, cooled in an ice bath until precipitation started to form with color changing, and then permitted to stand for over 6 hours. To get rid of any unreacted components, the solid complexes were separated and washed with a small amount of hot diluted ethanol. Vacuum desiccator was then used to dry the compounds (when varied colors of precipitate were gained) with a production rate of 77%. The complexes fragment at the range between 123 – > 300 °C. Scheme 1 shows how the ligand and metal ions complexes are created. The ligand and its metal complexes' analytic and physical characteristics are included in Table 1.

RESULTS AND DISCUSSION

Data on physical and analytical properties for the ligand and the synthesized complexes

The synthetic compounds illustrated in Scheme 1 were generated through the reaction of metal salts and ligand. Elemental analysis results indicate that all compounds exhibit a 1:2 (M:L) stoichiometry. These findings align with the theoretical calculations. Additionally, the conductivity measurements revealed that all the complexes are non-electrolytic, as shown in Table 1.

Table 1. Some elemental physical characteristics investigations of ligand and complexes.

Formula Molecular weight	m.p. °C		C %	H%	N%	M%	Cl%	Conductivity in DMSO $cm^2\ \Omega^{-1}mol^{-1}$
$C_{19}H_{16}N_4O$ 316.13	105-110	Calculated	72.13	5.10	5.10	-	-	-
		Found	(71.66)	(4.51)	(4.51)			
$C_{38}H_{30}N_8O_3V$ 697.19	>300	Calculated	65.42	4.33	16.06	7.30	-	21
		Found	(66.08)	(3.94)	(17.03)	(6.55)		
$C_{38}H_{32}ClCrN_8O_3$ 735.17	123-126	Calculated	62.00	4.38	15.22	7.06	4.82	10
		Found	(61.52)	(3.71)	(16.31)	(7.94)	(3.97)	
$C_{38}H_{30}MoN_8O_4$ 760.14	>300	Calculated	60.16	3.99	14.77	12.65	-	13
		Found	(59.43)	(4.62)	(15.64)	(13.37)		
$C_{38}H_{34}MnN_8O_4$ 721.21	200-207 decompose	Calculated	63.24	4.75	15.53	7.61	-	18
		Found	(64.08)	(5.01)	(16.39)	(6.65)		
$C_{38}H_{34}CuN_8O_4$ 729.20	180-185	Calculated	62.50	4.69	15.34	8.70	-	14
		Found	(61.67)	(4.03)	(16.88)	(7.98)		

Ligand and some products in the LC mass spectrometry

Mass spectrometry is a key analytical tool used to determine the molecular weight of the synthesized azo dye and its complexes by analyzing the mass-to-charge (m/z) ratio of ions, providing direct identification of molecules. The mass spectrum of ligand (Figure 2) shows the peak of the molecular ion $C_{10}H_8N_2O^+$ at m/z = 316.28 and its abundance of about 8%. In addition to other plenty for the rest of the pieces including $C_9H_5N^{\cdot+}$, $C_8H_6N^+$, and $C_2H_4N_2^+$.Their brilliance denotes the stability of the parts. In the mass spectrum of the VO^{+2} complex shown in (Figure 3), the complex moiety $C_{38}H_{30}N_8O_3V$ exhibited a peak at m/z 697.65, which corresponds to the expected mass of the complex. Additional peaks were observed at m/z 146.06, 143.04, 130.07, 116.05, 110.98, and 54.02, corresponding to fragment ions such as $C_9H_8NO^+$, $C_9H_5NO^{\bullet+}$, $C_9H_8N^+$, $C_8H_6N^+$, $CH_4N_2OV^+$, and $C_2H_2N_2^{\bullet+}$ at various intensities, indicating the fragmentation pattern of the complex. The Mo^{+6} complex exhibits a molecular ion peak at m/z 758.67 with a relative abundance of 10%. The fragmentation pattern corresponds to various fragment ions, including $C_9H_8N^+$, MoO_2, $C_7H_6NO^+$, $C_8H_6N^+$, $C_5H_5N_2O^+$, $C_6H_6N^+$, and $C_3H_5N_2^+$, appearing at m/z values of 130.17, 129.90, 120.04, 116.05, 109.04, 92.05, and 69.04, respectively. The mass spectrum of the Cr^{+3} exhibits a molecular ion peak at m/z 717.15 with a relative abundance of 9%. The fragmentation pattern corresponds to various fragment ions, including $C_{38}H_{32}ClCrN_8O_3$, $C_9H_5ClCrNO^+$, $C_{10}H_9N_3^{\cdot+}$, $C_9H_8N^+$, C_7H_6NO+, $C_3H_4N_2^{\cdot+}$ appearing at m/z values of 736.17, 229.95, 171.08, 130.17, 120.04, 68.04, respectively [17-19]. In Scheme 2, proposed fragmentation pathways and structural identification of fragments are presented.

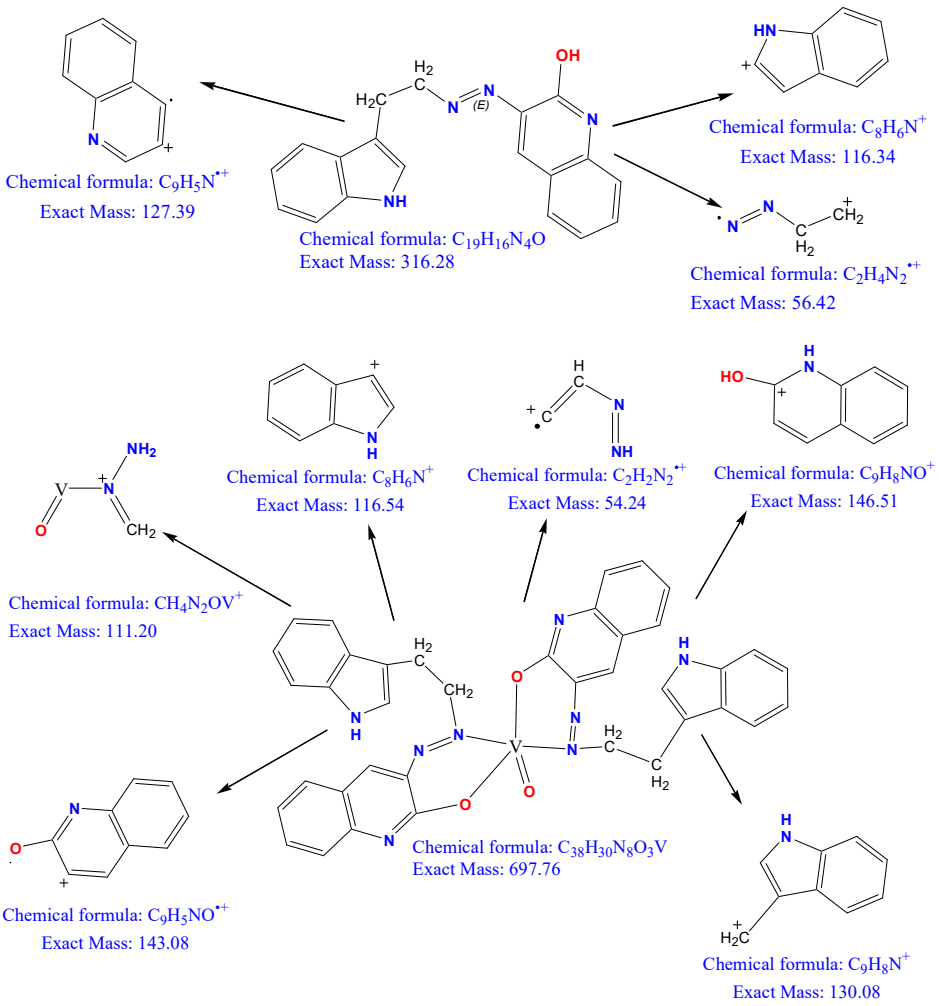
Chemical formula: $C_9H_5N^{\bullet+}$
Exact Mass: 127.39
Chemical formula: $C_{19}H_{16}N_4O$
Exact Mass: 316.28
Chemical formula: $C_8H_6N^+$
Exact Mass: 116.34
Chemical formula: $C_2H_4N_2^{\bullet+}$
Exact Mass: 56.42
Chemical formula: $C_8H_6N^+$
Exact Mass: 116.54
Chemical formula: $C_2H_2N_2^{\bullet+}$
Exact Mass: 54.24
Chemical formula: $C_9H_8NO^+$
Exact Mass: 146.51
Chemical formula: $CH_4N_2OV^+$
Exact Mass: 111.20
Chemical formula: $C_{38}H_{30}N_8O_3V$
Exact Mass: 697.76
Chemical formula: $C_9H_5NO^{\bullet+}$
Exact Mass: 143.08
Chemical formula: $C_9H_8N^+$
Exact Mass: 130.08

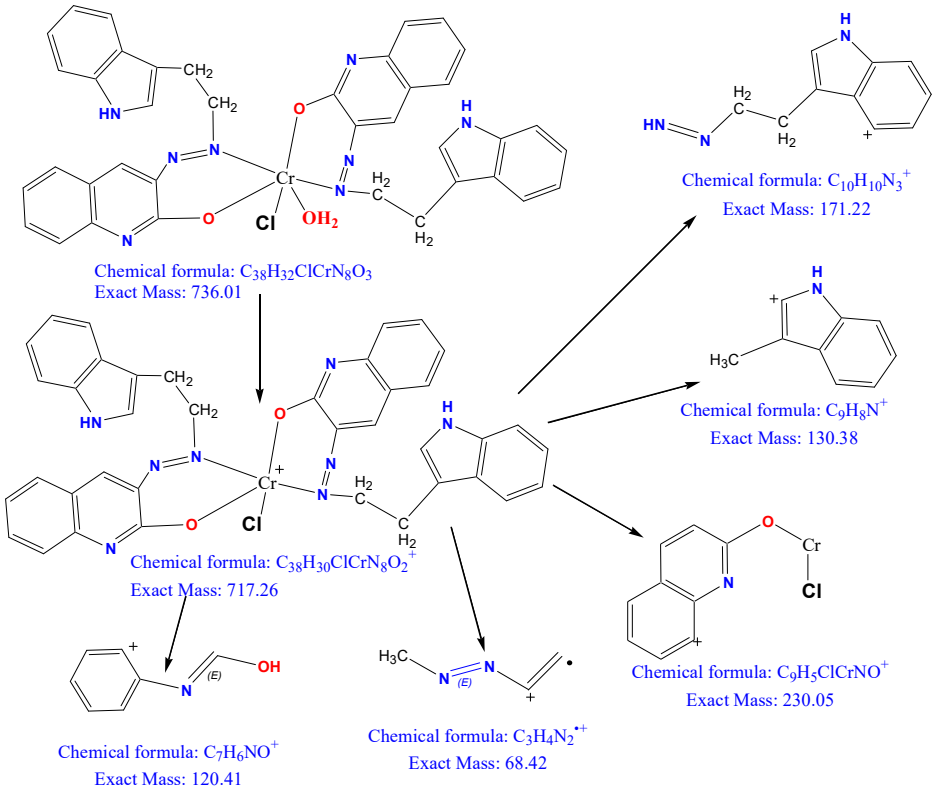
Chemical formula: $C_{38}H_{32}ClCrN_8O_3$
Exact Mass: 736.01
Chemical formula: $C_{38}H_{30}ClCrN_8O_2^+$
Exact Mass: 717.26
Chemical formula: $C_{10}H_{10}N_3^+$
Exact Mass: 171.22
Chemical formula: $C_9H_8N^+$
Exact Mass: 130.38
Chemical formula: $C_9H_5ClCrNO^+$
Exact Mass: 230.05
Chemical formula: $C_7H_6NO^+$
Exact Mass: 120.41
Chemical formula: $C_3H_4N_2^{\bullet+}$
Exact Mass: 68.42

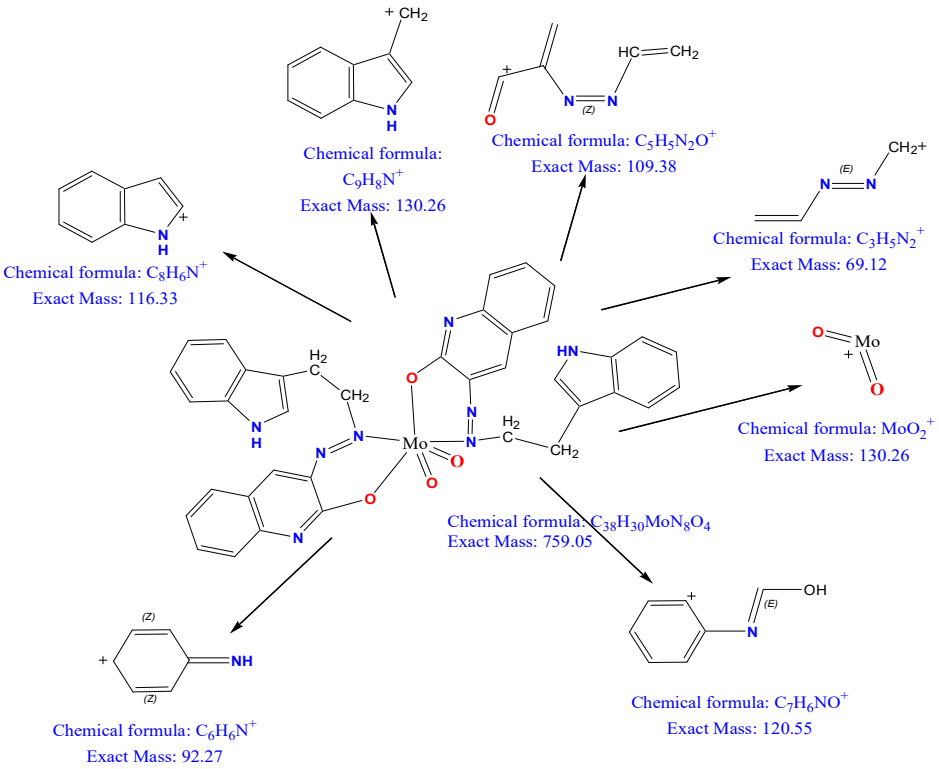

Scheme 2. Fragmentation of ligand, VO-complex, Cr-complex and Mo-complex.

Electronic spectra for compounds

The electronic spectrum of the ligand (HL) in Table 2 shows a strong absorption at (278 nm, 35971.2 cm^{-1}) and (337 nm, 29673.5 cm^{-1}) due to the π⟶π* transition and a peak at (340 nm, 29411.7 cm^{-1}) attributed to the n⟶π* transition, where a high intensity band is formed with an absorption maximum [20]. The electronic transition of VO^{+2} complex shown in Table 2, which peaks of (270, 330, 530 and 600) nm assigned to π→π*, n→ π*, $^2B_2g\rightarrow{}^2Eg$, $^2B_2g\rightarrow{}^2B_1g$, respectively, which is indicative of a square pyramidal geometry. The electronic absorptions of Cr^{+3}complex shown in Table 2 which peaks of (280, 320, 481, 609 and 667) nm ascribed to the π→π*, n→π*, $^4A_2g\rightarrow{}^3T_1g_{(p)}$, $^4A_2g\rightarrow{}^3T_1g_{(F)}$ and $^4A_2g\rightarrow{}^3T_2g_{(F)}$, respectively, which is an indicative of a octahedral. The electronic absorption of Mo^{6+} complex shown in Table 2 exhibited peaks of (260, 340 and 405) nm ascribed to the π→π*, n→π*, C.T. L→M, respectively, which is an indicative of a octahedral. The electronic absorption of Mn^{2+}complex shown in Table 2 exhibited peaks of (280, 365, 540, 630 and740) nm ascribed to the π→π*, n→π*, $^6A_1g\rightarrow{}^4A_1g$, $^4Eg(G)$, $^6A_1g\rightarrow{}^4T_2g(G)$ and $^6A_1g\rightarrow{}^4T_1g(G)$, respectively, which is an indicative of a octahedral. The electronic transition of Cu^{+2} complex shown in Table 2 which depicts a peak of (264, 328 and 519) nm ascribed to the π→π*, n→π*and $^2Eg\rightarrow{}^2T_2g$, respectively, it depicts an octahedral geometry [21-26] shown in the Table 2.

Table 2. Electronic spectral data (ultraviolet and visible) for ligands in their free-state and complexes and molar conductivity in DMSO (1×10^{-3} M) and magnetic susceptibility values.

Compound	λ nm	ύcm^{-1}	Abs	ε_{max}Lmol^{-1} cm^{-1}	Assignment	μ_{eff} (B.M)	Hybridization
Ligand	278	35971.2	1.7	1700	π→π*		
	337	29673.5	1.65	1650	π→π*		
	340	29411.7	1.6	1600	n→π*C.T		
[VO(L)$_2$]	270	37037.03	1.34	1340	π→π*	1.901	dsp^3
Square pyramidal	330	30303.03	1.02	1020	n→π *		
	530	18867	0.05	50	$^2B_2g \rightarrow {}^2Eg$		
	600	16666	0.1	100	$^2B_2g \rightarrow {}^2B_1g$		
[Cr(L)$_2$(H$_2$O)Cl]	280	35814.28	1.05	1050	π→π*	4.015	d^{2}sp^3
Octahedral	320	31250.0	1.44	1440	n→π *		
	481	20790.02	0.05	500	$^4A_2g \rightarrow {}^3T_1g$ (p)		
	609	16420.36	0.04	400	$^4A_2g \rightarrow {}^3T_1g$ (F)		
	667	14992.50	0.10	100	$^4A_2g \rightarrow {}^3T_2g$ (F)		
[Mo(L)$_2$O$_2$]	260	38461.53	1.25	1250	π →π*	diamag	d^{2}sp^3
Octahedral	340	29411.76	0.07	700	n→ π*	netic	
	405	24691.35	1.23	1230	C.T L→M		
[Mn(L)$_2$(H$_2$O)]	280	35714.28	0.975	975	π→π*	5.025	sp^{3}d^2
Octahedral	365	27397.26	0.050	500	n→π *		
	540	18518.51	0.023	23	$^6A_1g \rightarrow {}^4A_1g, {}^4Eg_{(G)}$		
	630	15873.01	0.024	24	$^6A_1g \rightarrow {}^4T_2g_{(G)}$		
	700	14285.71	0.025	25	$^6A_1g \rightarrow {}^4T_1g_{(G)}$		
[Cu(L)$_2$(H$_2$O)]	264	37878.78	1.45	1450	π→π*	1.902	sp^{3}d^2
Octahedral	328	30387.80	1.46	1460	n→π *		
	519	19267.82	0.05	500	$^2Eg \rightarrow {}^2T_2g$		

Thermal analysis

The detailed results of the thermal decomposition of the ligand and complexes are shown in Table 3 and Scheme 3 shows the stages of decomposition and the DSC results are shown in Table 3 showing the values of ΔH, ΔS, ΔG. Table 4 shows the thermogravimetric analysis of the ligand and complexes and showed the (Figure 4) for curve TGA and DSC for ligand. The results of thermogravimetric decomposition were interpreted according to Scheme 3, which resulted in the decomposition of the ligand in one stage, and the remainder was carbon, while the two complexes were decomposed in three stages. The first stage included the loss of the two water molecules, and the final remainder was the oxidation of the metal for both of them [27-33].

Table 3. DSC analysis of thermal decomposition for the ligand and several complexes.

compound	T_i /°C	T_f°C	Maximum temperature point °C	ΔH J/g	ΔS J	ΔG J	Type
HL	68.29	126.07	99.29	- 89.98	- 1.5572	64.634	Endothermic
$C_{38}H_{30}N_8O_3V$	47.16	65.49	56.56	-1.66	0.0905	-6.7786	Exothermic
	63.84	96.83	74.36	-26.45	0.8017	-86.064	Exothermic
	178.41	252.74	225.45	55.84	-0.7512	225.202	Endothermic
	325.45	339.59	334.57	-2.75	0.1948	-67.924	Exothermic
$C_{38}H_{32}ClCrN_8O_3$	41.08	106.52	66.81	-50.45	0.7709	-101.95	Exothermic
	127.85	172.88	150.79	-27.08	0.6013	- 117.27	Exothermic
	182.36	196.21	189.75	-1.19	0.0859	-17.489	Exothermic
	218.64	305.41	254.77	238.78	-2.7518	939.85	Endothermic
$C_{38}H_{30}MoN_8O_4$	48.01	108.52	67.26	-38.85	0.6420	-82.03	Exothermic

	123.85	178.87	155.79	-18.28	0.3322	-70.03	Exothermic
	186.36	198.21	188.78	-1.89	0.1594	-31.98	Exothermic
	215.64	308.21	257.47	257.38	-2.7803	973.22	Endothermic
$C_{38}H_{34}MnN_8O_4$	44.36	108.13	73.42	186.32	-2.9217	400.83	Endothermic
	213.42	358.93	288.39	258.99	-1.7798	772.26	Endothermic
$C_{38}H_{34}CuN_8O_4$	385.75	398.38	393.99	-3.97	0.3143	-127.801	Exothermic

Table 4. TGA data of the ligand and complexes.

Complex	step	T*i* °C	T*f* °C	Weight mass loss%	Reaction
HL	1	161.057	593.333	Calc. Found 96.162% 95.991%	- $C_{18}H_{16}N_4O$ C
Calculated:	96.162%	Final = 3.838%	Estimated: 95.991%		Final = 4.008%
$C_{38}H_{30}N_8O_3V$	1 2 3	78.627 213.231 360.477	213.231 360.477 577.89	15.849% 15.849% 58.157% 60.792% 23.522% 26.278%	-C_6H_9NO -$C_{20}H_{15}N_6O$ -$C_{12}H_6N$
					VO^{+2}
Calculated: 97.528 %		Final = 2.47%	Estimated: 102.9 %		Final = -2.9%
$C_{38}H_{32}ClCrN_8O_3$	1 2 3 4	56.968 168.471 242.1 389.359	168.471 242.1 389.359 594.409	7.26734% 7.9699% 6.1127% 6.1372% 60.8555% 61.167% 16.4645% 16.4660%	-H_2O/-Cl -C_2H_4OH -$C_{30}H_{18}N_5$ -C_6H_7O
					CrO^{+}
Calculated: 90.7010%		Final = 9.299%	Estimated = 91.73%		Final = 8.26%
$C_{38}H_{30}MoN_8O_4$	1 2 3	78.452 191.152 431.193	191.152 431.193 572.439	7.381% 7.332% 33.216% 33.132% 42.4432% 43.919%	-2CO -$C_{16}H_{18}N_3$ -$C_{20}H_{12}N_5$
					MoO_2^{+2}
Calculated: 83.039 %		Final = 16.961%	Estimated = 84.383 %		Final = 15.617%
$C_{38}H_{34}MnN_8O_4$	1 2	96.378 317.175	317.175 590.731	16.500% 17.011% 73.626% 74.341%	-$2H_2O$/- C_4H_4NOH -$C_{34}H_{25}N_7$ MnO
Calculated: 90.126 %		Final = 9.87 %	Estimated: 91.352 %		Final = 8.64%
$C_{38}H_{34}CuN_8O_4$	1 2 3	57.729 218.288 372.922	218.288 372.922 576.99	11.091% 11.318% 36.423% 36.682% 41.490% 41.188%	-$2H_2O$/-C_2H_4OH $C_{16}H_{18}N_4$ -$C_{20}H_7N_4$
					CuO
Calculated: 89.004 %		Final = 10.996 %	Estimated = 89.188 %		Final = 10.812 %

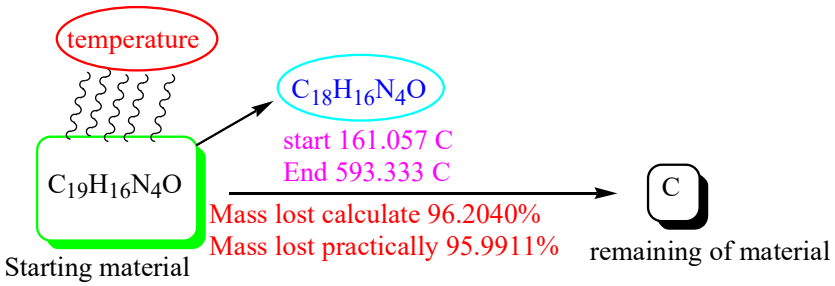
temperature
$C_{18}H_{16}N_4O$
start 161.057 C
End 593.333 C
$C_{19}H_{16}N_4O$
C
Mass lost calculate 96.2040%
Mass lost practically 95.9911%
Starting material
remaining of material

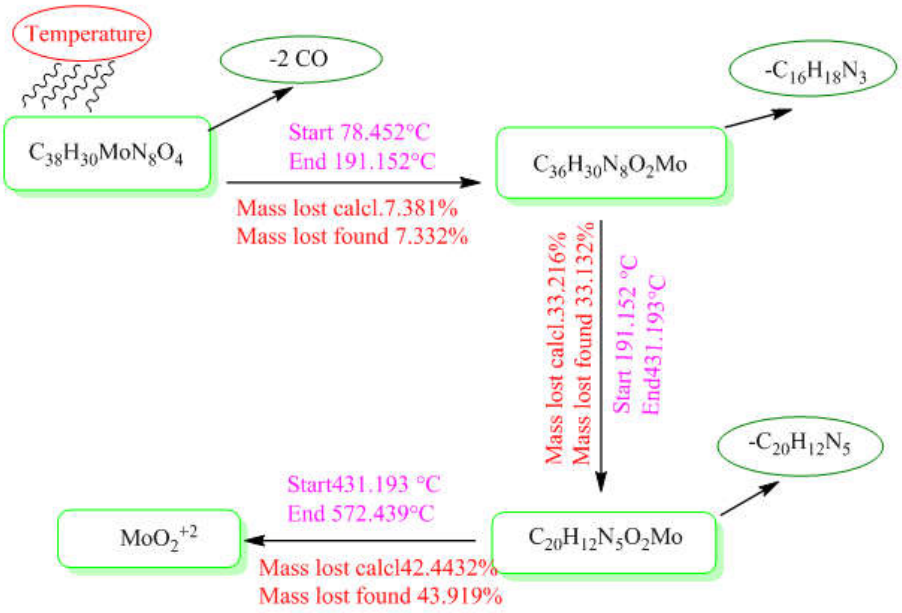
Temperature
-2 CO
$-C_{16}H_{18}N_3$
$C_{38}H_{30}MoN_8O_4$
Start 78.452°C
End 191.152°C
$C_{36}H_{30}N_8O_2Mo$
Mass lost calcl.7.381%
Mass lost found 7.332%
Mass lost calcl.33.216%
Mass lost found 33.132%
Start 191.152 °C
End431.193°C
$-C_{20}H_{12}N_5$
Start431.193 °C
End 572.439°C
MoO_2^{+2}
$C_{20}H_{12}N_5O_2Mo$
Mass lost calcl42.4432%
Mass lost found 43.919%

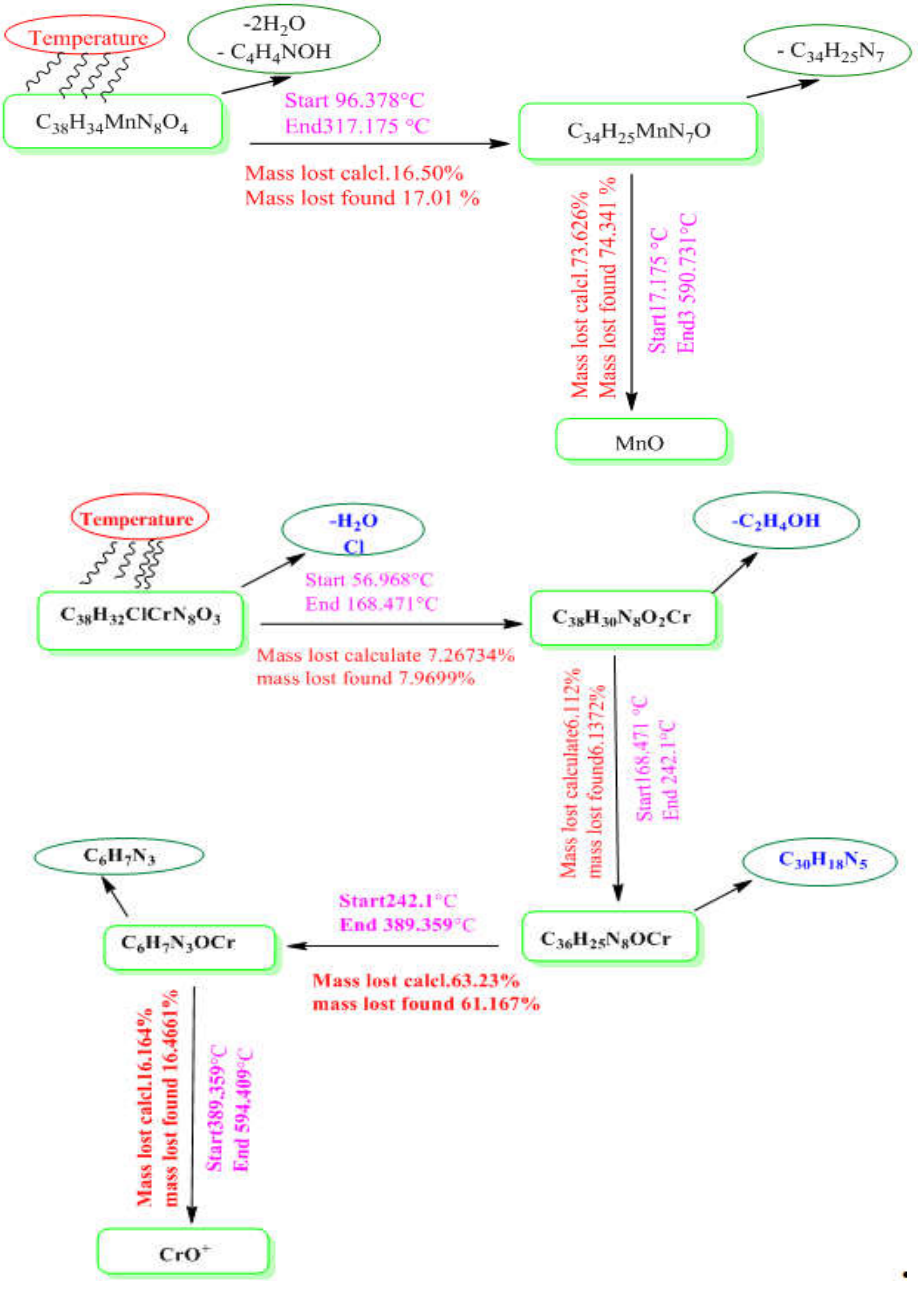
Temperature
-2H2O
- C4H4NOH
C38H34MnN8O4
Start 96.378°C
End317.175 °C
Mass lost calcl.16.50%
Mass lost found 17.01 %
C34H25MnN7O
- C34H25N7
Mass lost calcl.73.626%
Mass lost found 74.341 %
Start17.175 °C
End3 590.731°C
MnO
Temperature
-H2O
Cl
Start 56.968°C
End 168.471°C
C38H32ClCrN8O3
Mass lost calculate 7.26734%
mass lost found 7.9699%
C38H30N8O2Cr
-C2H4OH
Mass lost calculate6.112%
mass lost found6.1372%
Start168.471 °C
End 242.1°C
C6H7N3
C30H18N5
Start242.1°C
End 389.359°C
C6H7N3OCr
C36H25N8OCr
Mass lost calcl.63.23%
mass lost found 61.167%
Mass lost calcl.16.164%
mass lost found 16.4661%
Start389.359°C
End 594.409°C
CrO+

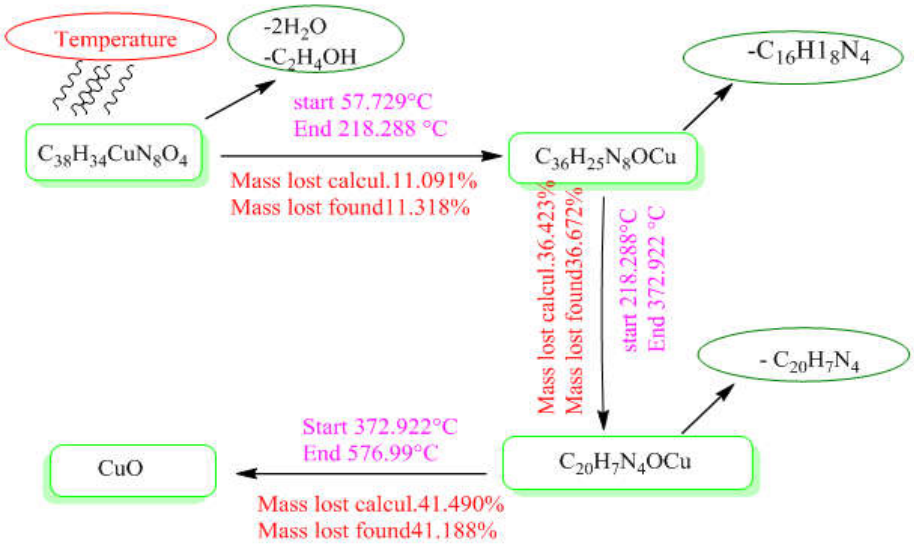

Scheme 3. Preliminary breakdown reactions of metal complexes and their ligand.

Infrared spectra

The infrared spectral data for the synthesized azo dye ligand and its corresponding metal complexes are provided in Table 5. It shows bands at 3304, 3191.82 cm^{-1} (O-H), and (NH) indole rings, respectively and at 1419.61 cm^{-1} corresponds to the new Azo group (N=N), confirming the formation of the ligand [34-38].Conversely the FT-IR spectra of the VO^{+2} , Mo^{+6}, Cu^{+2}, Mn^{+2} and Cr^{+3} complexes show the disappearance of the O-H stretching vibration of the phenolic group, which was in the free ligand Coordination occurs through the phenolic oxygen. Other evidence supporting the occurrence of coordination includes new vibrational modes corresponding to M-N, M-O, and V=O groups in the ranges of 572.66, 479.85, and 993.34 cm^{-1}, respectively. Additionally, changes in the shape, intensity, and position of the N=N mode, compared to that of the free ligand, further support coordination. Additionally, the stretching vibrational bands observed at (3491, 1641, and 754) cm^{-1} are attributed to the coordinated water molecules associated with the Cr-Cl, as reported in previous studies [39, 40]. These characteristic vibrations confirm the interaction between water molecules and the metal center. All Fourier transform infrared (FTIR) data, including these key vibration modes, are summarized in Table 5.

Table 5. Infrared spectral bands of ligand and their complexes (cm^{-1}).

Compounds	ν(H_2O) aqua δ(H_2O)	Other brands	υ (N=N)	ν(CH) arom. ν(CH) alph.	ν(NH) indol
(HL)	-	C-OH Phenolic 3304	1419.61	3049.46 2918.30	3191.82
$[VO(L)_2]$	-	572.66 ν(M-N), 479.85 ν (M-O), 993.34 ν(M=O	1467.11	3019.60 2927.16	3199.58
$[Cr(L)_2(H_2O)Cl]$	3491.21 1641.42 754.17	619.15 ν(M-N), 503.43 ν(M-O), 451.34ν (Cr-Cl)	1460.11	3049.46 2926.01	3186.82
$[Mo(L)_2O_2]$	-	572.86 ν(M-N), 499.56	1402.25	3028.24	3188.11

		ν(M-O), 1115 ν(O=Mo=O) (Cis)		2910.0	
$[Mn(L)_2(H_2O)]$	3414.00 1641.42 835.18	501.49ν (M-N), 457.13 ν(M-O),	1458.18	3020.13 2900.1	3201.83
$[Cu(L)_2(H_2O)]$	3412.08 1645.28 756.10	497.63ν (M-N), 462.92 ν(M-O),	1467.83	3024.46 2926.01	3183.40

Antioxidant activity

Antioxidants effectively neutralize DPPH free radicals by donating hydrogen atoms. The stable DPPH radical can accept an electron from a hydrogen atom, forming a diamagnetic molecule. The reduction in DPPH concentration is measured by the decrease in absorbance at 517 nm due to antioxidants [41, 42]. The results of the antioxidant analysis showed that the azo ligand (HL) and its metal complexes under study, namely VO^{+2} , Mo^{+6}, Cu^{+2}, $Mn^{+2}$and Cr^{+3}, possess antioxidant properties when compared to ascorbic acid.it was found that the ligand is more effective at removing free radicals, largely due to the presence of a hydroxyl group [35, 38]. Consequently, when the sample solution is introduced, the free radicals are neutralized by the sample, which donates either a hydrogen atom or an electron, leading to the neutralization of the free radicals. As a result, the sample produces fewer free radicals. The outcomes were as follows (Gallic acid > $[Cr(L)_2(H_2O)$ Cl] > $[Mn(L)_2(H_2O)]$ > $[VO(L)_2]$ > Ligand = $[Mo(L)_2O_2]$ > $[Cu(L)_2(H_2O)]$) as illustrated in Table 6 variations of IC_{50} values for Gallic acid its compounds .

Table 6. The antioxidant results (P1%, RSA% and IC_{50}) of ligand and their metal complexes.

compound	Concentration µg/mL	PI%	RSA%	IC_{50} µg/mL
Gallic acid	0.008	11.39	88.61	0.855
	0.004	27.79	72.21	
	0.002	36.49	63.51	
	0.001	40.12	59.88	
	0.0005	43.18	56.82	
Ligand	0.008	48.41	51.59	1.001
	0.004	55.92	44.08	
	0.002	59.76	40.24	
	0.001	63.06	36.94	
	0.0005	63.46	36.54	
$[VO(L)_2]$	0.008	23.33	76.67	0.908
	0.004	37.05	62.95	
	0.002	46.16	53.84	
	0.001	48.67	51.33	
	0.0005	53.39	46.61	
$[Cr(L)_2(H_2O)Cl]$	0.008	11.16	88.84	0.869
	0.004	51.16	48.84	
	0.002	55.39	44.61	
	0.001	60.29	39.71	
	0.0005	61.06	38.94	
$[Mo(L)_2O_2]$	0.008	20.71	79.29	1.001
	0.004	29.79	70.21	
	0.002	36.49	63.51	
	0.001	40.12	59.88	
	0.0005	41.18	58.82	
$[Mn(L)_2(H_2O)]$	0.008	32.09	67.91	0.899
	0.004	38.92	61.08	
	0.002	45.06	54.94	

	0.001 0.0005	48.97 49.78	51.03 50.22	
$[Cu(L)_2(H_2O)]$	0.008 0.004 0.002 0.001 0.0005	11.61 23.06 30.34 35.33 37.06	88.39 76.94 69.66 64.67 62.94	1.012

Investigation of anticancer activity

Cancer cell growth was determined using MTT, and MCF7 cells were digested with trypsin. The cells were treated with 20-320 µg/mL(five concentration) with compounds for 24 hours at 37 °C in 5% CO_2, and the MTT solution was added in phosphate-buffered saline for an additional four hours, and the absorbance was determined as 570 nm. Using an ELISA reader, and the concentration of compounds Cu-Complex, Mo-Complex, ligand in Table 7, that led to 50% of cell death was determined, the results showed that the inhibition was high for the compounds, as the highest inhibition was for Mo complex, followed by ligand and Cu complex according to the IC_{50} value. When compared to healthy cells. Also, the percentage of free radical inhibition of these compounds was molybdenum, which gave the highest inhibition, followed by ligand, then cupper. These compounds were chosen over others based on studies and references that advise preferring these minerals over others due to their vital importance. [37-42], along with the IC_{50} values. Illustrate the cell viability rates in MCF-7 cells treated with the chosen compounds. It is clear from the displayed figures that our compounds have behavior against MCF-7 according to the order Mo-complex > HL > Cu-complex.

Table 7. Cellular toxicity of compounds towards MCF-7.

Sample	Ligand					MCF-7/24H
Construction (µg/mL)	0	20	40	80	160	320
Absorption at 570 nm	1.123/1.125/1.098	0.7105/0.7104/0.7191	0.6326/ 0.6412/ 0.6259	0.611/0.5421/0.5736	0.3793/0.3582/0.3599	0.1014/0.1027/0.0743
Viability (%)	98.38157	63.00342	54.30128	49.41799	29.46467	2.798008
Average viability (%)	100	62.46499	54.98599	49.60162	30.01556	4.525366
Standard deviation(±)	1.404704	0.466324	0.716119	3.220549	1.09451	1.497166
Sample	Mo-complex					MCF-7/24h
Construction (µg/mL)	0	20	40	80	160	320
Absorption at 570 nm	1.123 1.125 1.098	0.625 0.687 0.644	0.4632 0.4323 0.4543	0.2745 0.2545 0.2789	0.154 0.1706 0.1614	0.102 0.1143 0.1124
Viability (%)	98.382	55.991	38.279	21.902	10.931	6.3554
Average viability (%)	100	56.738	37.871	21.005	10.987	6.0909
Standard deviation(±)	1.4047	2.9659	1.4852	1.2142	0.7765	0.6182
Sample	Cu-complex					MCF-7/24h

Construction (µg/mL)	0	20	40	80	160	320
Absorption at 570 nm	1.123 1.125 1.098	0.9165 0.9264 0.9451	0.8386 0.8572 0.8619	0.7875 0.7181 0.7496	0.5553 0.5346 0.5359	0.2804 0.2787 0.2503
Viability (%)	98.382	84.105	76.337	65.851	45.898	19.231
Average viability (%)	100	82.633	75.465	66.05	46.461	21.052
Standard deviation(±)	1.4047	1.3561	1.1505	3.2446	1.0825	1.5788

CONCLUSION

In summary, using a straightforward substitution process using 2-hydroxyquinoline, we were able to successfully synthesize a novel azo ligand derivative with tryptamine. Then, ligand and metal the complexes were identified using various analytical methods, including thermal analysis curves (TGA and DSC), elemental microanalysis, metal chlorides, conductivity measurements, magnetic susceptibility, ^{1}H and ^{13}C NMR, FT-IR and UV-Vis spectroscopy. Thermodynamic parameters ΔH, ΔS and ΔG were calculated using DCS curves. The bidentate coordination sites of atoms N and O in the ligand were identified by comparing the infrared spectra with those of the metal complexes. The M:L ratio of each compound was [1:2]. The dye was used to determine its ability to inhibit free radicals using its prepared complexes, and its ability as an antioxidant was determined using DPPH as a free radical and gallic acid as a standard substance, The IC_{50} value was determined and it was found that the ligand had high free radical inhibition ability. The free radical inhibition ability and complex inhibition ability changed according to the IC_{50} value, and the results were as follows (Gallic acid > $[Cr(L)_2(H_2O)Cl]$ > $[Mn(L)_2(H_2O)]$ > $[VO(L)_2]$ > ligand = $[Mo(L)_2O_2]$ > $[Cu(L)_2(H_2O)]$), ligand, Cu^{+2}, and Mo^{+6} complexes were evaluated as anticancer agents breast cancer MCF-7 in five concentrations, the results showed that the IC_{50} value for ligand was 49.86 µg/mL, while the Mo complex gave 25.48 µg/mL, Cu complex gave 123.8 µg/mL, meaning that the Mo-complex gave a higher inhibition value than ligand and Cu.

REFERENCES

1. Mohammed, H.S. Synthesis, characterization, structure determination from powder X-ray diffraction data, and biological activity of azo dye of 3-aminopyridine and its complexes of Ni(II) and Cu(II). *Bull. Chem. Soc. Ethiop*. **2020**, 34, 523-532.
2. Dakiky, M.; Nemcova, I. Aggregation of O,O′-dihydroxy azo dyes III. Effect of cationic, anionic and non-ionic surfactants on the electronic spectra of 2-hydroxy-5-nitrophenylazo-4-[3-methyl-1-(4″-sulfophenyl)-5-pyrazolone]. *Dyes Pigm*. **2000**, 44, 181-193.
3. Mezgebe, K.; Mulugeta, E. Synthesis and pharmacological activities of azo dye derivatives incorporating heterocyclic scaffolds. A review. *RSC Adv*. **2022**, 12, 25932-25946.
4. Reda, S.M.; Al-Hamdani, A.A.S. Synthesis, characterization, thermal analysis and bioactivity of some transition metals complexes with new azo ligand. *Chem. Methodol*. **2022**, 6, 475-493.
5. Al-Resayes, S.I.; Jarad, A.J.; Al-Zinkee, J.M.; Al-Noor, T.H.; El-ajaily, M.M.; Abdalla, M.; Min, K.; Azam, M.; Mohapatra, R.K. Synthesis, characterization, antimicrobial studies, and molecular docking studies of transition metal complexes formed from a benzothiazole-based azo ligand. *Bull. Chem. Soc. Ethiop*. **2023**, 37, 931-944.
6. Patra, A.K.; Nethaji, M.; Chakravarty, A.R. Synthesis, crystal structure, DNA binding and photo-induced DNA cleavage activity of (S-methyl-l-cysteine) copper(II) complexes of heterocyclic bases. *J. Inorg. Biochem*. **2007**, 101, 233-244.

7. Al-Daffay, R.K.H; Al-Hamdani, A.A.S. Synthesis and characterization of some metals complexes with new acidicazo ligand 4-[(2-amino-4-phenylazo)-methyl]-cyclohexane carboxylic acid. *Iraqi J. Sci*. **2022**, 63, 3264-3275.
8. Nakbi, H.; Dallel, W.; Hammami, S.; Mighri, Z. Phytochemical profile and antioxidant properties of leaves extracts from *Posidonia oceanica* (L.) Delile and their allelopathic potential on terrestrial plant species. *Bull. Chem. Soc. Ethiop*. **2020**, 34, 437-447.
9. Al-Daffay, R.K.H.; Al-Hamdani, A.A.S. Synthesis, characterization, and thermal analysis of a new acidicazo ligand's metal complexes. *Baghdad Sci. J*. **2023**, 20, 121-133.
10. Hirano, R.; Sasamoto, W.; Matsumoto, A.; Itakura, H.; Igarashi, O.; Kondo, K. Antioxidant ability of various flavonoids against DPPH radicals and LDL oxidation. *J. Nutr. Sci. Vitaminol*. **2001**, 47, 357-362.
11. Mohammed, H.; Al-Hasan, H.; Chaieb, Z.; Zizi, Z.; Abed, H. Synthesis, characterization, DFT calculations and biological evaluation of azo dye ligand containing 1,3-dimethylxanthine and its Co(II), Cu(II) and Zn(II) complexes. *Bull. Chem. Soc. Ethiop*. **2023**, 37, 347-356.
12. Al-Hamdani, A.A.S.; Al-Zahraa, F.SH.H.; Mutar, S.A.; Mohammed, N.U.G. Synthesis and characterization of new (Au, Ru and Rh) ion complexes and evaluating their activity as anticancer and antioxidants. *Appl. Biochem. Biotechnol.* **2025**, doi: 10.1007/s12010-024-05140-w.
13. Jirjees, V.Y.; Al-Hamdani, A.A.S.; Wannas, N.M.; Dib, A.; Al Zoubi, W. Spectroscopic characterization for new model from Schiff base and its complexes. *J. Phys. Org. Chem.***2021**, 34, e4169.
14. Zafar, S.; Bukhari, D.A.; Rehman, A. Azo dyes degradation by microorganisms–An efficient and sustainable approach. *Saudi J. Biol. Sci*. **2022**, 29, 103437.
15. Shahi, N.; Shah, S.K.; Yadav, A.P.; Bhattarai, A. Micellization pattern of cationic surfactants in presence of azo dye in methanol mixed media. *Results Chem*. **2023**, 5, 100906.
16. Alhalafi, M.H. Novel azo-dye quinazolinones as colorimetric chemosensors for detection of cobalt and ferrous ions in aqueous medium. *J. Saudi Chem. Soc*. **2023**, 27, 101685.
17. Ravi, B.N.; Keshavayya, J.; Kumar, V.; Kandgal, S. Synthesis, characterization and pharmacological evaluation of 2-aminothiazole incorporated azo dyes. *J. Mol. Struct*. **2020**, 1204, 127493.
18. Agwamba, E.C.; Udoikono, A.D.; Louis, H.; Udoh, E.U.; Benjamin, I.; Igbalagh, A.T.; Ushaka, U.B. Synthesis, characterization, DFT studies, and molecular modeling of azo dye derivatives as potential candidate for trypanosomiasis treatment. *Chem. Phys. Impact* **2022**, 4, 100076.
19. Asiri, S.; Kassem, M.A.; Eltaher, M.A.; Saad, K.M. Novel coordination compounds based on copper complexes with new synthesized Schiff bases and azo-dyes as sensitizers for dye-sensitized solar cells: Spectral and electrochemical studies. *Int. J. Electrochem. Sci*. **2020**, 15, 6508-6521.
20. Obaid, S.M.H.; Jarad, A.J.; Salih Al-Hamdani, A.A. Synthesis, characterization and biological activity of mixed ligand metal salts complexes with various ligands. *J. Phys.: Conf. Ser*. **2020**, 1660, 012028.
21. Venugopal, N.; Krishnamurthy, G.; Bhojyanaik, H.S.; Krishna, P.M. Synthesis, spectral characterization and biological studies of Cu(II), Co(II) and Ni(II) complexes of azo dye ligand containing 4-amino antipyrine moiety. *J. Mol. Struct*. **2019**, 1183, 37-51.
22. Prashantha, G.; Keshavayya, J.; Ali, R.S. Synthesis, spectral characterizations and biological applications of novel 3-[(E)-(4,6-dihydroxy pyrimidin-5-yl) diazenyl]-4-methylbenzoic acid azo dye and their derivatives. *Results Chem*. **2021**, 3, 100110.
23. Wannas, N.M; Al-Hamdani, A.A.S.; Al Zoubi, W. Spectroscopic characterization for new complexes with 2,2′-(5,5-dimethylcyclohexane-1,3-diylidene)bis(azan-1-yl-1-ylidene) dibenzoic acid. *J. Phys. Org. Chem*. **2020**, 33, e4099.

24. Akram, D.; Elhaty, I.A.; AlNeyadi, S.S. Synthesis and spectroscopic characterization of rhodanine azo dyes as selective chemosensors for detection of iron(III). *Chem. Data Collect*. **2020**, 28, 100456.
25. Al Zoubi, W.; Al-Hamdani, A.A.S.; Widiantara, I.P.; Hamoodah, R.G.; Ko, Y.G. Theoretical studies and antibacterial activity for Schiff base complexes. *J. Phys. Org. Chem*. **2017**, 30, e3707.
26. Abd El-Lateef, M.; Khalaf, M.; Amer, A.; Kandeel, M.; Abdelhamid, A.; Abdou, A. Synthesis, characterization, antimicrobial, density functional theory, and molecular docking studies of novel Mn(II), Fe(III), and Cr(III) complexes incorporating 4-(2-hydroxyphenylazo)-1-naphthol (Az). *ACS Omega* **2023**, 8, 25877-25891.
27. Al Zoubi, W.; Jirjees, V.; Suleman, V.; Kim, Y.G.; Ko, Y.G. Synthesis and bioactivity studies of novel Schiff bases and their complexes. *J. Phys. Org. Chem*. **2019**, 32, e4004.
28. El-Ghamry, H. A.; Alkurbi, A. A.; Alhasani, M. A.; Takroni, K. M.; Khedr, A. M. Copper-based azo dye catalysts for phenoxazinone synthase mimicking efficiency: Structure characterization and bioactivity evaluation. *Arab. J. Chem*. **2023**, 16, 104916.
29. Ren, H.; Li, F.; Yu, S.; Wu, P. The detection of multiple analytes by using visual colorimetric and fluorometric multimodal chemosensor based on the azo dye. *Heliyon* **2022**, 8, 1-12.
30. El-Ghamry, H.A.; Alkurbi, A.A.; Alhasani, M.A.; Takroni, K. M.; Khedr, A.M. Copper based azo dye catalysts for phenoxazinone synthase mimicking efficiency structure characterization and bioactivity evaluation. *Arab J. Chem*. **2023**, 16,8, 104916,
31. Keshavayya, J. Synthesis, structural investigations and in vitro biological evaluation of N,N-dimethyl aniline derivatives based azo dyes as potential pharmacological agents. *J. Mol. Struct*. **2019**, 1186, 404-412.
32. Obaid, S.M.H.; Sultan, J.S.; Al-Hamdani, A.A.S. Synthesis, characterization and biological efficacies from some new dinuclear metal complexes for base 3-(3,4-dihydroxy-phenyl)-2-[(2-hydroxy-3-methylperoxybenzylidene)-amino]-2-methyl propionic acid. *Indones. J. Chem.* **2020**, 20, 1311-1322.
33. Reda, M.M.; Mohammed, L.A. Preparation, characterization and studied biological effect as antioxidant of azo compound and Schiff base complexes. *J. Surv. Fish. Sci*. **2023**, 10, 1144-1156.
34. Sarvalkar, P.D.; Jamadar, A.S.; Magdum, A.B.; Pawar, P.K.; Yadav, J.B.; Nimbalkar, M. S.; Sharma, K. K. Biogenic synthesis of Co_3O_4 nanoparticles from Aloe barbadensis extract: Antioxidant and antimicrobial activities, and photocatalytic degradation of azo dyes. *Results Eng*. **2024**, 22, 102094.
35. Hamza, I.S.; Mahmmoud, W.A.; Al-Hamdani, A.A.; Allaf, A.W.; Al Zoubi, W. Synthesis, characterization, and bioactivity of several metal complexes of (4-amino-N-(5-methyl-isaxazol-3-yl)-benzenesulfonamide). *Inorg. Chem. Commun*. **2022**, 144, 109776.
36. Jirjees, V.Y.; Suleman, V.T.; Al-Hamdani, A.A.S.; Ahmed, S.D. Preparation, spectroscopic characterization and theoretical studies of transition metal complexes with 1-[(2-(1H-indol-3-yl)ethylimino)methyl]naphthalene-2-ol ligand. *Asian J. Chem*. **2019**, 31, 2430-2438.
37. Reda, S.M.; Al-Hamdani, A.A.S. Mn(II), Fe(III), Co(II) and Rh(III) complexes with azo ligand: Synthesis, characterization, thermal analysis and bioactivity. *Baghdad Sci. J*. **2023**, 20, 642-660.
38. Hekal, H.A.; Kassab, R.M.; Abd El Salam, H.A.; Shaban, E.; Atlam, F.M. Synthesis, computational studies, molecular docking, anti-inflammatory and antioxidant activities of α-aminophosphonates incorporating an azo chromophore for polyester printing application. *ChemistrySelect* **2023**, 8, e202204075.
39. Al-Zahraa, F.S.H.H.; Al-Hamdani, A.A.S. Synthesis, characterization, thermal studies, and antioxidant activities of azo dye [2-[(3-hydroxyphenyl)diazinyl]-1,2-benzothiazol-3(2h)-one-1,1-dioxide] and metal ion complexes. *Iraqi J. Sci*. **2024**, 65, 6842-6861.

40. Fadhel, A.M.; Al-Hamdani, A.A.S.; Mohamed, S.G. Synthesis, characterization and antioxidant study of some metal ion complexes with azo 1-(2,4,6-trihydroxy-3-((3-hydroxyphenyl) diazenyl) phenyl) ethan-1-one. *Baghdad Sci. J*. **2024**, 21, 3642-3660.
41. Abdullah, A.M.; Al-Hamdani, A.A.S. Synthesis, characterization, thermal studies and antioxidant activities of transition metal complexes with azo dye ligand. *Baghdad Sci. J.***2024**, 21, 1512-1535.
42. Al-Rubaye, N.T.A; Al-Hamdani, A.A.S. Synthesis, characterization, of some metal ion complexes with new azo dye and studying antioxidant and anticancer (MCF-7). *Bull. Chem. Ethiop.* **2025**, 39, 859-875.